Available online at www.sciencedirect.com
ScienceDirect
International Journal of Mass Spectrometry 268 (2007) 47–59
International Journal of Mass Spectrometry
www.elsevier.com/locate/ijms

Study of factors governing negative molecular ion yields of amino acid and peptide in FAB, MALDI and ESI mass spectrometry

Takashi Nishikaze, Mitsuo Takayama *

International Graduate School of Arts and Sciences, Yokohama City University, Yokohama 236-0027, Japan

Received 19 May 2007; received in revised form 5 August 2007; accepted 11 August 2007
Available online 17 August 2007

Abstract

The factors governing negative and/or positive molecular ion yields of amino acids and peptides in the soft ionization methods of fast atom bombardment (FAB), matrix-assisted laser desorption/ionization (MALDI) and electrospray ionization (ESI) mass spectrometry have been examined. The results obtained have been interpreted from the standpoint of two different components, namely desorption and ionization, by relating the ion yields to physicochemical properties of amino acid and peptides. The negative-ion yields of amino acids in FAB were found to be dependent on gas-phase acidity and aliphatic/hydrophobicity. In MALDI, a linear correlation was observed between negative-ion yields and gas-phase acidity of amino acids. In both FAB and MALDI mass spectra of peptides, the presence of aspartic acid residues tended to enhance the negative-ion yields. The presence of aliphatic/hydrophobic residues in FAB or aromatic amino acid residues in MALDI enhanced the negative-ion yields of peptides. In ESI, the charge state distributions of multiply-protonated peptides were dependent on the number of basic sites and their position in the sequence, while those of multiply-deprotonated peptides were dependent on the number of acidic sites. The total ion yields in ESI were governed by hydrophobicity of peptides and efficiency of acquiring the charge(s). The results suggest that the ion yields were governed by two independent processes, namely ionization and desorption, regardless of the ionization methods used.

Keywords: Negative-ion yield; FAB; MALDI; ESI; Peptide

1. Introduction

Mass spectrometry (MS) has been used as a powerful analytical method for investigating various kinds of analytes such as organic and inorganic compounds. The advent of soft ionization methods such as matrix-assisted laser desorption/ionization (MALDI) [1–3] and electrospray ionization (ESI) [4,5] has allowed the development of MS techniques into more sensitive analytical tools allowing analysis without decomposition of large and fragile molecules such as peptides, proteins and other biological polymers. Mass spectrometers equipped with these soft and sensitive ionization sources have became indispensable tools for identification of proteins expressed by genomes [6]. In practice, peptide-mass fingerprinting [7,8] and amino acid sequencing by tandem mass spectrometry [9,10] have become common approaches for the characterization of proteins and determination of post-translational modifications.

Although protein and peptide analysis using soft ionization has commonly been performed in positive-ion mode because of its superior ion yields compared to the negative-ion mode, simultaneous use of positive- and negative-ion mode often provides useful information in protein identification and in screening for phosphorylated sequences in protein digests. Bigwarfe and Wood [11] have reported that using negative-ion MALDI and ESI of protein digests results in the detection of a number of peaks in the mass spectra that are not observed in positive-ion mode, and that greater sequence coverage and improved database search scores are obtained by combining the positive- and negative-ion data. Janek et al. [12] have reported that phosphorylated peptides, which give small ion yields in positive-ion mode, exhibit improved signal intensities in negative-ion mode, and that comparative measurements using positive- and negative-ion MALDI-MS provide a simple and rapid method for screening for phosphorylated sequences in protein digests.

* Corresponding author. Present address: International Graduate School of Arts and Sciences, Yokohama City University, 22-2 Seto, Kanazawa-ku, Yokohama, Kanagawa 236-0027, Japan. Tel.: +81 45 787 2431; fax: +81 45 787 2317.
E-mail address: takayama@yokohama-cu.ac.jp (M. Takayama).

1387-3806/$ – see front matter © 2007 Elsevier B.V. All rights reserved.
doi:10.1016/j.ijms.2007.08.004

These reports indicate that the use of negative-ion mode provides important and valuable information in protein identification.

Regardless of whether positive- or negative-ion mode has been used, if all peaks from protein digests are observed as the molecular-related ion peaks $[M+H]^+$ or $[M-H]^-$ in mass spectra, accurate protein identification would be possible. However, the molecular ion yields of peptides are strongly dependent on their intrinsic physicochemical properties which are a result of the individual properties of the side chains of the constituent amino acids. Amino acids have a wide variety of physicochemical properties such as acidity, basicity, hydrophobicity associated with aliphatic or aromatic character and hydrophilicity associated with the acidic or basic nature and with the presence of other functional groups such as hydroxyl and thiol groups. Recent reports have suggested that several intrinsic properties of peptides influence their molecular ion yields in MALDI-MS. It has been reported that the presence of Arg, aliphatic, and aromatic amino acids residues enhance the ion yields of peptides in positive-ion mode in MALDI-MS [13–16], while little information is available concerning negative-ion mode. Bigwarfe and Wood [11] have pointed out that peptides from digests rich in Asp and Glu residues tend to give more prominent signals in negative-ion mode. Despite a good deal of work in the area [11,12], the relationship between the ion yields and physicochemical properties of analyte remains unclear for negative ion experiments. The molecular ion yields are of practical importance, as well as being of fundamental interests in MS.

We recently reported [16] that physicochemical factors of individual amino acids cooperatively affected the ion yields of protonated amino acids and peptides $[M+H]^+$ in the desorption/ionization methods MALDI and fast atom bombardment (FAB). In order to relate the ion yields to the physicochemical factors such as basicity and hydrophobicity, the total ionization processes were divided into two different components, desorption and ionization. These two processes are quite different with desorption being a physical process which forms gaseous species from the condensed-phase, while ionization is a thermochemical process which forms molecular-related ions such as $M^{\bullet+}$, $[M+H]^+$, and $[M-H]^-$. In conventional methods such as electron ionization and chemical ionization, the total ionization processes can be clearly divided into physical vaporization and thermochemical ionization components. For MS ionization techniques, it is also useful to divide the total ionization processes into two processes, namely gaseous species formation and ionization. In order to understand the ion yields in soft ionization MS, here we use a constitutional form where we have divided the total ionization processes J_i into ionization efficiency of molecules I and the rate of desorption or vaporization of neutral molecules J_v as follows:

$$J_i = IJ_v \quad (1)$$

The efficiency I can be related to thermochemical quantities such as proton affinity, gas-phase basicity, ionization energy or electron affinity of a given analyte. The quantity J_v represents the ability of analyte molecules to desorb or vaporize from condensed- to gas-phase. The aim of this paper is to investigate factors governing the molecular ion yields in negative-ion mode in the soft ionization methods of FAB, MALDI and ESI.

2. Experimental

2.1. Materials

The angiotensin- and bradykinin-related peptides were purchased from Peptide Institute (Osaka, Japan). The sequences are summarized in Table 1, with the hydrophobicity index which has been derived using the data of Bull and Breeze

Table 1
Angiotensin- and bradykinin-related peptides used

Analyte peptide	Monoisotopic mass (Mm)	Sequence											Hydrophobicity index[a]
Angiotensin1 (A1)	1295.677	D	R	V	Y	I	H	P	F	H	L		−429
[Val5]-Angiotensin1 (A2)	1281.662	D	R	V	Y	V	H	P	F	H	L		−359
Angiotensin2 (A3)	1045.593	D	R	V	Y	I	H	P	F				−416
[Val5]-Angiotensin2 (A4)	1031.519	D	R	V	Y	V	H	P	F				−329
[Asn1,Val5]-Angiotensin2 (A5)	1030.535	N	R	V	Y	V	H	P	F				−294
Angiotensin (human1-7) (A6)	898.466	D	R	V	Y	I	H	P					−259
Des-Asp1-[Ile8]-Angiotensin2 (A7)	896.523		R	V	Y	I	H	P	I				−553
Angiotensin3 (A8)	930.507		R	V	Y	I	H	P	F				−563
Angiotensin4 (A9)	774.406			V	Y	I	H	P	F				−772
Bradykinin (B1)	1059.561			R	P	P	G	F	S	P	F	R	−104
[Tyr8]-Bradykinin (B2)	1075.556			R	P	P	G	F	S	P	Y	R	−94
Des-Pro2-Bradykinin (B3)	962.509				R	P	G	F	S	P	F	R	−96
Des-Arg9-Bradykinin (B4)	903.406			R	P	P	G	F	S	P	F		−204
Des-Arg9-[Leu8]-Bradykinin (B5)	869.476			R	P	P	G	F	S	P	L		−220
Lysyl-Bradykinin (Kallidin) (B6)	1187.656		K	R	P	P	G	F	S	P	F	R	−48
Tyrosyl-Bradykinin (B7)	1222.625		Y	R	P	P	G	F	S	P	F	R	−238
Des-Arg10-Kallidin (B8)	1031.555		K	R	P	P	G	F	S	P	F		−130
Methionyl-Lysyl-Bradykinin (B9)	1318.697	M	K	R	P	P	G	F	S	P	F	R	−104
Isoleucyl-Seryl-Bradykinin (B10)	1259.677	I	S	R	P	P	G	F	S	P	F	R	−179

[a] Obtained by addition of ΔF values for individual amino acids taken from Ref. [17], each sum being divided by the number of amino acids in the peptide.

[17]. All amino acids except for glutamic acid were purchased from Sigma–Aldrich (Steinheim, Germany). Glutamic acid was purchased from Wako Pure Chemical (Osaka, Japan). The FAB matrix chemicals *m*-nitrobenzyl alcohol (*m*NBA), dithiothreitol (DTT) and diethanolamine (DEA) were purchased from Tokyo Kasei (Tokyo, Japan). The MALDI matrix chemical α-cyano-4-hydroxycinnamic acid (CHCA) was purchased from Sigma–Aldrich (Steinheim, Germany). Trifluoroacetic acid (TFA), acetonitrile (HPLC Grade) and distilled water (HPLC Grade) were purchased from Wako Pure Chemical (Osaka, Japan). All reagents were used without further purification.

2.2. FAB-MS

FAB mass spectra were acquired on a JEOL JMS-700 MStation reverse geometry double-focusing mass spectrometer (JEOL Ltd., Tokyo, Japan). The FAB gun was operated at 5 kV and 10.4 mA of current using Xe as the fast atom. The spectra were obtained in negative ion mode. The acceleration potential and mass resolution were set to 10 kV and 2000 (10% valley definition), respectively. Each analyte (amino acid or peptide) was dissolved in water at a concentration of 10 nmol/μL and 2 μL of analyte solution was mixed with 8 μL of matrix consisting of a 1:1 (v/v) mixture of *m*NBA and DTT (*m*NBA/DTT) or DEA. A volume of 2 μL of the solution was deposited onto a FAB stainless probe tip. The reproducibility of spectral patterns was confirmed over scans 1–10, and the spectra were averaged over scans 3–8. The standard deviation of the peak intensity for molecular-related ions was estimated from the spectra obtained.

The ion yields (Y) of $[M-\mathrm{H}]^-$ ions of amino acids and peptides were estimated as the ratio of $[M-\mathrm{H}]^-$ intensity to that for the matrix ions. For *m*NBA/DTT matrix, the negative molecular ions *m/z* 153, $\mathrm{B_1}^{\bullet -}$ for *m*NBA and *m/z* 153, $[\mathrm{B_2}-\mathrm{H}]^-$ for DTT were used as follows:

$$Y(\%) = 100 \times \frac{I[M-\mathrm{H}]^-}{I[\mathrm{B_1}^{\bullet -}] + I[\mathrm{B_2}-\mathrm{H}]^-}$$

In DEA matrix, deprotonated DEA dimer (*m/z* 209, $[2\mathrm{B}-\mathrm{H}]^-$) was used in the ratio as follows:

$$Y(\%) = 100 \times \frac{I[M-\mathrm{H}]^-}{I[2\mathrm{B}-\mathrm{H}]^-}$$

2.3. MALDI-TOFMS

MALDI-TOF mass spectra were acquired using an AXIMA-CFR instrument (Shimadzu Corp., Kyoto, Japan). A nitrogen laser (337 nm) was used to irradiate the sample for ionization. The spectra were obtained in negative-ion reflectron mode for amino acids and linear mode for peptides. The acceleration potential was set to 20 kV using a gridless-type electrode. Each amino acid or peptide analyte was dissolved in water at a concentration of 1 nmol/μL and 1 pmol/μL, respectively. Analyte solution (5 μL) was mixed with 5 μL of saturated solution of matrix in water/acetonitrile (1:1, v/v) with 0.1% TFA. A volume of 1 μL of sample solution was deposited onto a MALDI sample plate and the solvents were removed by allowing evaporation in air at room temperature. Spectra were the sum of 100 profiles automatically acquired rastering the sample spot. Each profile was the result of 12 consecutive single laser pulses for peptides, and five consecutive laser pulses for amino acids.

The ion yields (Y) of $[M-\mathrm{H}]^-$ ions of amino acids and peptides were estimated as the ratio of $[M-\mathrm{H}]^-$ intensity to that of the fragment ion of CHCA (*m/z* 93, $[\mathrm{B_{frag}}]^-$) as follows:

$$Y(\%) = 100 \times \frac{I[M-\mathrm{H}]^-}{I[\mathrm{B_{frag}}]^-}$$

2.4. ESI-MS

Each peptide was dissolved in 20% acetonitrile at a concentration of 2 pmol/μL. Five microliters of the solutions were injected into a Finnigan Surveyor LC system (Thermo Electron, Bremen, Germany), and the eluate was directed to the ESI interface of a Finnigan LCQ Advantage MAX ion trap mass spectrometer (Thermo Electron, Bremen, Germany). For all the ESI experiments described here, the total combined flow rate provided by two LC pumps was 100 μL/min. Pump A was used to deliver water, while pump B delivered acetonitrile. All full-scan mass spectra of peptides were obtained under isocratic conditions (acetonitrile/water ratio used was 20/80), without column and flow injection analysis of single components. Four replicate analyses were performed at room temperature.

The positive- and negative-ion yields of peptides were calculated using the following formula:

$$\sum [M+n\mathrm{H}]^{n+} \quad (n = 1-4),$$

$$\sum [M-n\mathrm{H}]^{n-} \quad (n = 1-2)$$

where $\sum$ is the sum of the areas under the curves of all charge states of the peptides. The ion yields of peptides were calculated as the mean of four measurements.

3. Results and discussion

3.1. Negative-ion yields of amino acids in FAB with mNBA/DTT matrix

The molecular ion yields obtained from FAB of amino acids are summarized in Table 2, together with values of gas-phase acidity (GA) [18,19] and Bull and Breeze (B&B) indices (ΔF) [17] of hydrophobicity. The B&B index has been widely used to represent hydrophobicity of amino acids and peptides, because the index reflects the surface concentration of amino acid solution. A higher concentration of amino acid on the surface would be expected to have higher capability to desorb or vaporize from the surface. In negative-ion FAB with *m*NBA/DTT matrix, acidic amino acids, Asp (0.92%) and Glu (0.82%), were detected with relatively high intensity. Medium ion yields were obtained for Asn (0.25%), Gln (0.34%), Leu (0.35%), Ile (0.22%) and Met (0.20%), while Trp, Thr, Cys and His gave yields lower than 0.13%. The peaks of Ser and His overlapped with the

Table 2
Ion yields $Y(\%)$ of $[M-H]^-$ measured for free amino acids in negative-ion FAB and MALDI, values of gas phase acidity [18], B&B hydrophobicity ΔF [17] and monoisotopic mass (Mm) of amino acids

Amino acids	Mm (u)	FAB (%) *m*NBA/DTT	FAB (%) DEA	MALDI (%)	GA (kcal/mol)	ΔF (kcal/mol)
Glu	147.05	0.82	1.80	=	[a]	0.51
Asp	133.04	0.92	0.77	84.2	319.1[b]	0.61
Arg	174.11	0.10	1.70	–	330.1	0.69
His	155.07	=	1.17	=	331.0[c]	0.69
Gln	146.07	0.34	1.62	=	331.0	0.97
Asn	132.05	0.25	=	29.4	331.7	0.89
Thr	119.06	0.13	1.60	28.2	331.7	0.29
Ser	105.04	=	=	16.4	332.0	0.42
Cys	121.02	0.13	–	36.4	332.9	0.36
Met	149.05	0.20	8.73	=	336.0	−0.66
Trp	204.09	0.12	1.58	=	337.7	−1.20
Tyr	181.07	–	1.30	4.8	337.7	−1.43
Lys	146.11	–	0.98	=	338.4	0.46
Val	117.08	–	2.80	8.6	338.7	−0.75
Ile	131.10	0.22	4.33	13.1	339.1	−1.45
Leu	131.10	0.35	4.97	12.3	339.1	−1.65
Phe	165.08	–	2.47	9.7	339.4	−1.52
Ala	89.05	–	1.00	4.6	340.0	0.61
Gly	75.03	–	0.16	4.4	340.1	0.81
Pro	115.06	–	1.50	=	340.8	−0.17

–: not detected. =: not estimated owing to overlap with intense matrix peaks.
[a] Not determined.
[b] Theoretical value [18].
[c] Value taken from Ref. [19].

intense background peaks originating from matrix ions. The other amino acids Phe, Tyr, Val, Pro, Lys, Ala and Gly did not show any molecular-related negative ions. The yields of deprotonated molecules $[M-H]^-$ observed in negative-ion FAB were plotted against the GA and B&B index of each amino acid as shown in Fig. 1(a) and (b), respectively. Fig. 1(a) does not include the acidic amino acid Glu, because gas-phase acidity of this amino acid has not been determined [17]. The higher ion yields of Asp and Glu can be attributed to their acidic nature. Although the value of GA for Glu has not been determined, it is expected that Glu has a large GA value in the region of that of Asp. This result suggests that GA is the dominant factor in the production of gas-phase negative ions $[M-H]^-$ under FAB conditions. Although Fig. 1(a) shows that increasing GA tends to increase ion yields for most amino acids, the data for Leu, Ile and Arg (enclosed within the left ellipse and center circle in Fig. 1(a)) deviates significantly from this tendency. Leu and Ile have relatively large hydrophobicity, while their GA values are relatively small. This indicates that the negative-ion yields are also governed by hydrophobicity to some extent. Note that

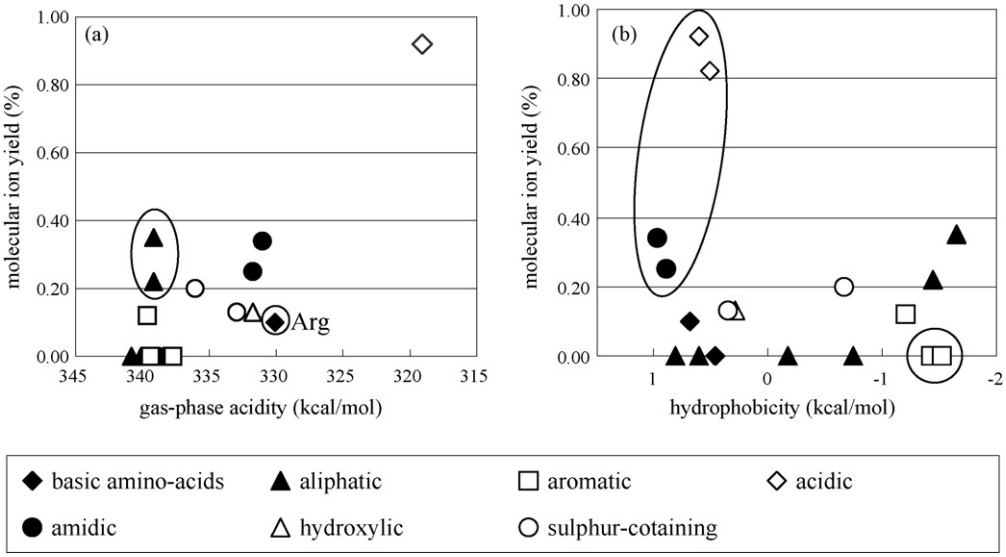

Fig. 1. Yields of deprotonated molecules $[M-H]^-$ of amino acids in negative-ion FAB with *m*NBA/DTT matrix. (a) Ion yields vs. gas-phase acidity and (b) ion yields vs. B&B hydrophobicity. The standard deviations for the yields were within 2–9% for all amino acids.

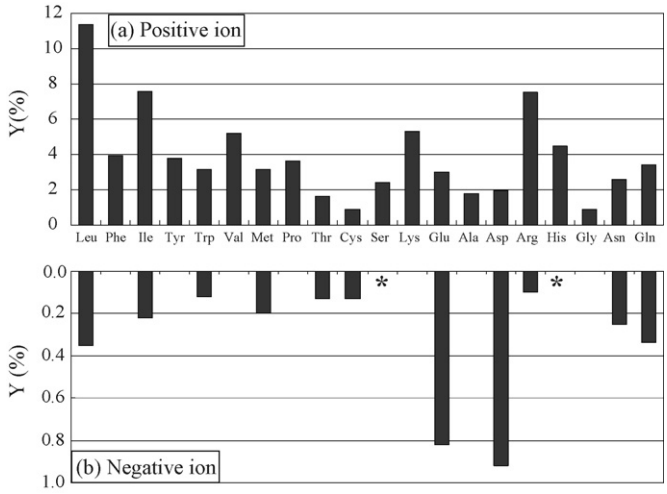

Fig. 2. Yields of molecular-related ions of amino acids in FAB. (a) Yields of protonated molecules $[M+H]^+$ in positive-ion FAB [16]. (b) Yields of deprotonated molecules $[M-H]^-$ in negative-ion FAB. Asterisks indicate that the ion yields could not be estimated owing to overlap within intense peaks originating from matrix.

Arg has outstanding proton affinity (PA), while its GA is relatively large. The outstanding PA of Arg is advantageous for producing the gas-phase protonated form, but is disadvantageous in the production of the gas-phase deprotonated form. This is clearly shown in Fig. 2 which displays the comparison between positive- and negative-ion yields of amino acids in FAB with *m*NBA/DTT matrix. In desorption/ionization methods, positive- and negative-ion formation occurs simultaneously and competitively.

Although hydrophobicity was expected to be one of the factors governing molecular ion yields in FAB, Fig. 1(b) does not demonstrate a reasonable positive correlation. Excluding the ellipse and circle areas, however, the negative-ion yields roughly increase with increasing hydrophobicity. The left ellipse area contains the acidic amino acids Asp and Glu and amidic amino acids Asn and Gln. These amino acids possess large GA values, while their hydrophobicities are small. The right circle area includes the aromatic amino acids Phe and Tyr. These amino acids possess relatively high hydrophobicity as indicated by the B&B index (Table 2), and did not give any molecular-related negative ions (Fig. 1(b)) These results indicate that aliphatic hydrophobicity of Leu and Ile is advantageous for producing gas-phase ions, but aromatic hydrophobicity of Phe and Tyr is not. As seen in Fig. 2, the positive effect of aliphatic hydrophobicity and the negative effect of aromatic hydrophobicity on the ion yields are in accord with the data obtained in positive-ion FAB [16]. It is expected that in general the surface concentration of these hydrophobic amino acids would be high, and that these amino acids are favorable for FAB-induced vaporization and thus give higher ion yields. This has been suggested by the reports of positive-ion FAB [20–24], and is in consistent with the 'bubble chamber model' for FAB events [25]. The results obtained here can be simply interpreted on the basis of the hypothesis [16] that total ionization process is governed by two processes, desorption and ionization and each can be considered independently. Thus, aliphatic hydrophobicity of Leu and Ile may increase the desorption term J_v in Eq. (1), and therefore enhance the ion yields in both positive- and negative-ion mode. The negative contribution of aromatic hydrophobicity of Phe and Tyr to the ion yields might be rationalized in terms of intermolecular interactions between aromatic π-electrons in the amino acids and in the matrix *m*NBA molecules, as well as in positive-ion mode [16]. However, this is not the case. These aromatic/hydrophobic amino acids also gave low ion yields using DEA matrix, where aromatic π-electrons are not involved, as described below.

3.2. Negative-ion yields of amino acids in FAB with basic DEA matrix

It is widely accepted that use of a basic matrix such as DEA is suitable for negative-ion FAB. Using DEA matrix, 17 amino acids could be detected at significant intensity (Table 2). The peaks of Ser and Asn could not be estimated owing to overlap with the intense background peaks originating from the DEA matrix. Only the thiol-containing amino acid Cys did not show any signals. The yields of deprotonated amino acids $[M-H]^-$ observed in negative-ion FAB using DEA matrix are plotted against the GA and B&B index of each amino acid in Fig. 3(a) and (b), respectively. Based on the results of negative-ion FAB using *m*NBA/DTT, aliphatic/hydrophobic amino acids and acidic amino acids were expected to give higher ion yields than others. As expected, aliphatic/hydrophobic amino acids Leu, Ile and Val gave higher ion yields than other relatively hydrophilic amino acids. In contrast to the measurements using *m*NBA/DTT, however, acidic Asp and Glu did not give higher ion yields. These unexpected results may be due to the basic nature of the DEA matrix. Basic DEA matrix can effectively extract protons from amino acids regardless of the acidity of analytes. Thus, DEA matrix may equalize the ionization efficiencies (I in Eq. (1)) of analyte amino acids. Thus, ion yields of amino acids using DEA matrix were only dependent on the desorption term J_v, which corresponds to the ability of analytes to vaporize from matrix surface to gas-phase. With the exception of Met and aromatic amino acids, the ion yields of amino acids in negative-ion FAB with DEA matrix showed reasonable dependence on hydrophobicity, as shown in Fig. 3(b). In particular, the ion yields of aliphatic amino acids (Gly, Ala, Pro, Val, Ile, and Leu; black triangle in Fig. 3(b)) increased linearly with their increasing hydrophobicity. This indicates that an aliphatic/hydrophobicity is the factor facilitating vaporization from the liquid matrix surface to gas-phase in negative-ion FAB using DEA matrix, as well as positive- and negative-ion FAB using *m*NBA/DTT matrix. The reason for the extremely high ion yield of Met is not immediately apparent. As discussed above, the aromatic/hydrophobic amino acids Phe, Tyr, and Trp provided lower ion yields than that expected from their hydrophobicity. These amino acids also gave low ion yields using DEA matrix, as seen enclosed within the circle in Fig. 3(b). The negative contribution of aromaticity to the ion yields may be explained by intermolecular interactions between aromatic π-electrons in the amino acids and π- and/or σ-electrons in the matrix molecules. These intermolec-

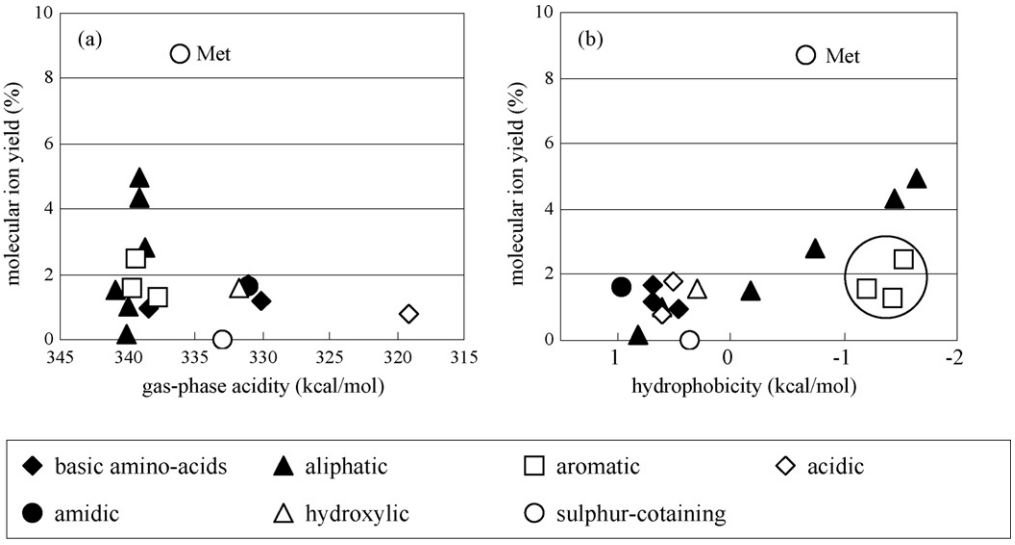

Fig. 3. Yields of deprotonated molecules $[M-H]^-$ of amino acids in negative-ion FAB with DEA matrix. (a) Ion yields vs. gas-phase acidity and (b) ion yields vs. B&B hydrophobicity. The standard deviations for the yields were within 4–9% for all amino acids.

ular interactions can contribute to the solubility leading to a decrease in surface concentrations of aromatic amino acids. The remarkable deviation of Met and aromatic amino acids from the positive correlation in Fig. 3(b) should be further investigated.

The results obtained using two different matrices, *m*NBA/DTT and DEA, indicate that the negative-ion yields of amino acids are governed not only by the physicochemical properties of analyte, but to some extent also by the characteristics of matrix used. The specific nature of matrix such as the basic properties of DEA can obscure the effects of acidity of analyte amino acids on negative-ion yields, as described above. While details of matrix effect on the ion yields are beyond the scope of this paper, it is important to take into account that the nature of matrix also affects the desorption and ionization process independently. The basic nature of DEA affects the ionization process, and may equalize the ionization efficiency (I in Eq. (1)) of analyte amino acids. In this sense, *m*NBA/DTT matrix is universal matrix, and is useful for study of factors governing molecular ion yields.

3.3. Negative-ion yields of amino acids in MALDI

In this study, we used CHCA matrix because CHCA is a conventional and widely used MALDI matrix which gives decreased formation of sweet spots compared to other matrices such as 2,5-dihydroxybenzoic acid, allowing comparison of quantitative results. Unfortunately, the ion yields of seven deprotonated amino acids Tyr, Met, Pro, Lys, Glu, His and Gln could not be estimated owing to overlap with the strong peaks originating from the CHCA matrix in negative-ion MALDI. Of those amino acids not overlapping with matrix ions the peak of deprotonated Arg could not be detected. The highest ion yield was obtained for Asp (64.5%). Thr (15.6%), Cys (23.4%), Ser (12.2%), and Asn (20.5%) could be detected in moderate abundance. Other amino acids gave ion yields of less than 10%. The high ion yield of Asp can be attributed to its acidic nature. Moderate ion yields of Thr, Cys, Ser and Asn are due to the presence of hydroxyl, thiol and amide groups that possess relatively high gas-phase acidity compared to other amino acids (see Table 2). Although the aliphatic/hydrophobic amino acids such as Val, Ile and Leu gave high ion yields under negative-ion FAB, these amino acids did not give high ion yields under negative-ion MALDI conditions. The lack of dependence of ion yields on aliphatic/hydrophobicity is presumably due to the fact that in MALDI the analyte molecules are incorporated into the solid matrix, while in FAB the analytes are dissolved in liquid matrix.

The yields Y of deprotonated amino acids $[M-H]^-$ observed in negative-ion MALDI are plotted separately against the gas-phase acidity and B&B hydrophobicity of each amino acid in Fig. 4(a) and (b), respectively. Fig. 4(a) shows a reasonably simple linear correlation between Y values and GA, with the exception of Arg. Arg has a relatively large GA value, but is the most basic amino acid of the 20 naturally occurring amino acids. The high basicity of Arg preferentially leads to the protonation reaction, so that the formation of deprotonated Arg is completely suppressed under MALDI conditions. In fact, Arg gave the highest ion yield in positive-ion MALDI [16], as shown in Fig. 5 that shows a comparison between positive- and negative-ion yields of amino acids. In contrast, the plot of Y against B&B hydrophobicity does not show any correlations, as seen in Fig. 4(b). This indicates that in negative-ion MALDI the ion yield of amino acids depends on their ionization efficiency I which directly relates to GA.

The results obtained from the negative-ion FAB and MALDI experiments with amino acids can be used to help understand the ion yields of peptides described below.

3.4. Negative-ion yields of peptides in FAB

The negative-ion yields Y of angiotensin- and bradykinin-related peptides in FAB were estimated using the ratio $I[M-H]^-/(I[B_1{}^{\bullet -}]+I[B_2-H]^-)$, and the yields were com-

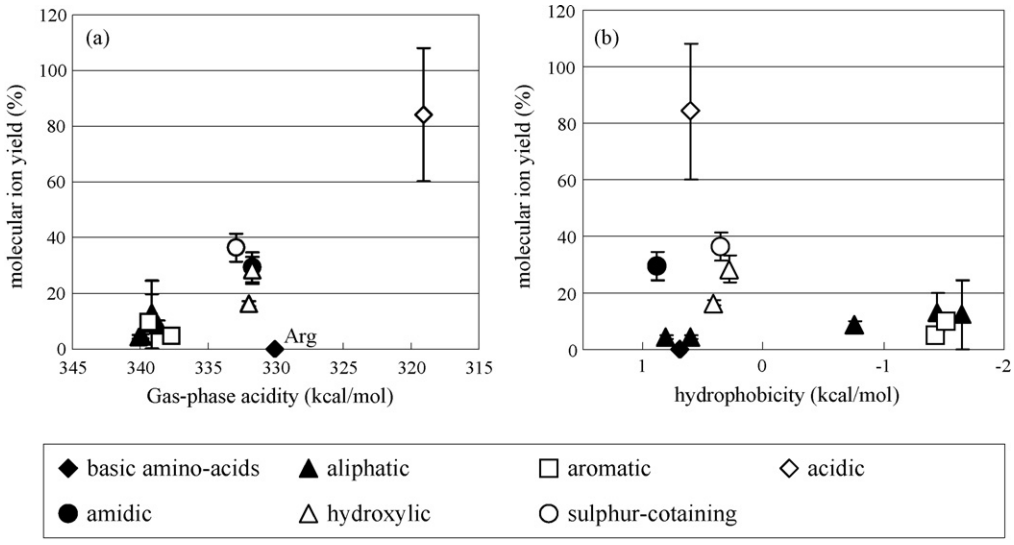

Fig. 4. Yields of deprotonated molecules $[M-H]^-$ of amino acids in negative-ion MALDI. (a) Ion yields vs. gas-phase acidity and (b) ion yields vs. B&B hydrophobicity.

pared with the positive-ion yields (Fig. 6). In negative-ion FAB with *m*NBA/DTT matrix, angiotensin1 (A1, 3.45%), [Val^5]-angiotensin1 (A2, 2.80%), des-Asp^1-[Ile^8]-angiotensin2 (A7, 2.18%), and angiotensin4 (A9, 2.77%) gave higher ion yields than seen for other angiotensin-related peptides. Angiotensin2 (A3, 0.93%) and angiotensin3 (A8, 1.09%) gave medium ion yields, and other peptides gave ion yields of less than 0.5%. Among the bradykinin-related peptides, the highest ion yield was obtained for des-Arg^9-[Leu^8]-bradykinin (B5, 2.46%). Medium ion yield was obtained with des-Arg^9-bradykinin (B4, 1.17%). Other peptides gave ion yields of less than 0.5%.

Comparison of the sequence of A1 and A2 indicates that the conversion of Val5 into Ile5 increased the ion yield from 2.80% to 3.45%. The same trend was observed in a comparison of A3 (Ile at position 5) which gave a yield of 0.93% and A4 (Val at position 5) which gave a yield of 0.46%. In addition, the conversion of Phe8 in A8 into Ile8 in A7 enhanced the *Y* value from 1.09% to 2.18%. Such a positive effect due to the presence of an aliphatic/hydrophobic residue such as Ile can also be observed in the conversion of Phe8 in B4 (1.2%) into Leu8 in B5 (2.5%). Whereas aliphatic/hydrophobic residues were advantageous for the production of negative ions of peptides under FAB conditions, in the comparison between A3 (0.9%) and A6 (0.6%), the aromatic/hydrophobic residue did not play an important role in generating gas-phase deprotonated peptides. The effects of aliphatic/hydrophobicity and aromatic/hydrophobicity on the ion yields can be seen in both positive- and negative-ion yields (Fig. 6). This figure indicates that the FAB ion yields of peptides are governed by surface activity which is directly related to aliphatic/hydrophobicity. The signal enhancement effects resulting from the aliphatic/hydrophobic nature of peptides is consistent with the results obtained from amino acids as described above. The positive influence of aliphatic/hydrophobic residues in peptides on the yields may be interpreted *via* the term corresponding to the rate of desorption J_v in Eq. (1). The influence of the ionization efficiency *I* which is related to acidic and basic nature will be described below.

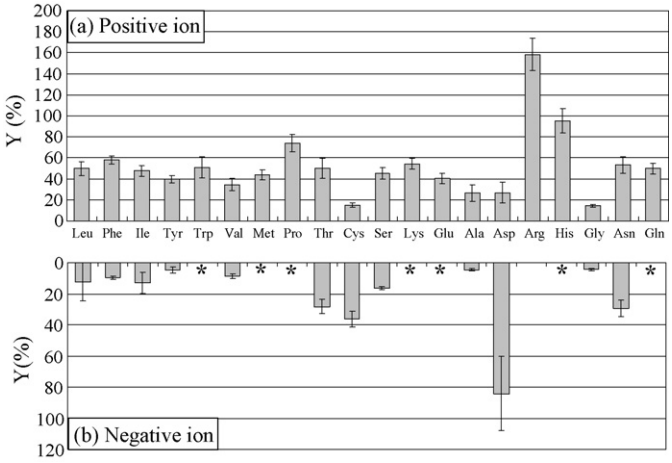

Fig. 5. Yields of molecular-related ions of amino acids in MALDI. (a) Yields of protonated molecules $[M+H]^+$ in positive-ion MALDI [16]. (b) Yields of deprotonated molecules $[M-H]^-$ in negative-ion MALDI. Asterisks indicate that the ion yields could not be estimated owing to overlap with intense peaks originating from matrix.

Fig. 6 demonstrates that in negative-ion FAB the yields of A7 (2.2%) and A8 (1.1%) are lower than that of A9 (2.77%), while the positive-ion data shows a trend in the opposite direction. The peptide A9 lacks an Arg residue compared to A7 and A8. There are two reasons why removal of the Arg residue enhances the yield of deprotonated peptides. First, the absence of the basic Arg residue decreases the formation of protonated peptides, so that a larger fraction of peptides would be shunted into the deprotonation reaction. The lack of the Arg residue would be advantageous for the formation of $[M-H]^-$ ions by means of the ionization efficiency *I* in Eq. (1). Second, the removal of the hydrophilic Arg residue contributes to an increase in hydrophobicity of peptides. It is likely that the higher ion yield obtained with A9 over

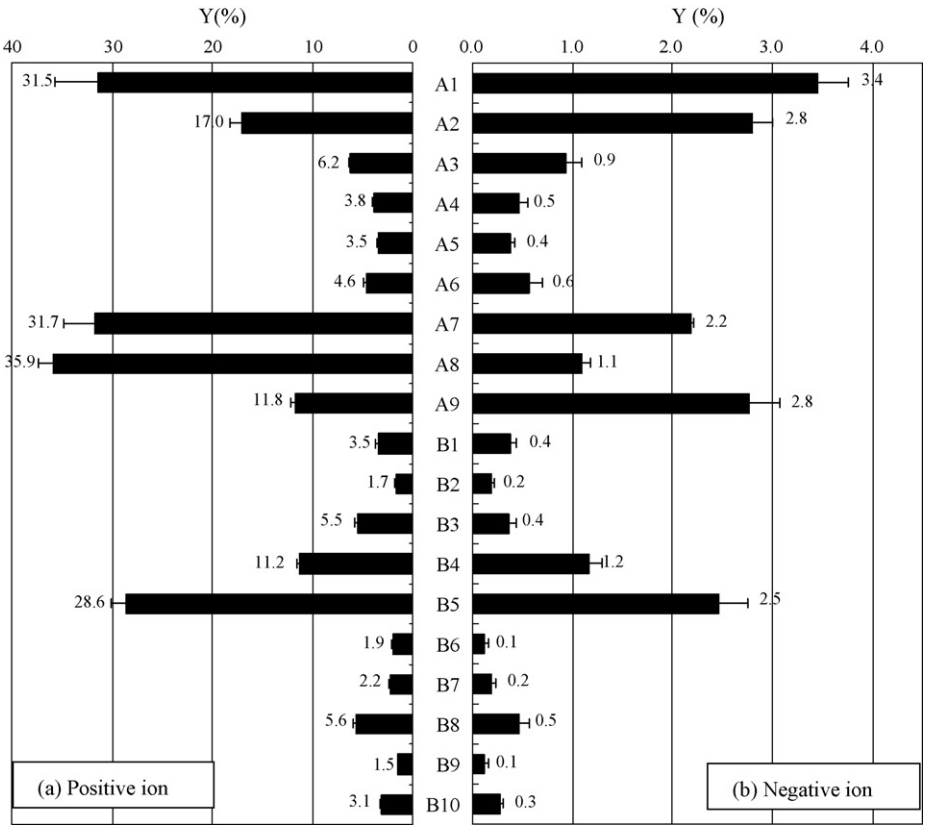

Fig. 6. Yields of molecular-related ions of angiotensin-related peptides (A1–A9) and bradykinin-related peptides (B1–B10) in FAB. (a) Yields of protonated molecules $[M+H]^+$ in positive-ion FAB [16]. (b) Yields of deprotonated molecules $[M-H]^-$ in negative-ion FAB.

that of A7 and A8 is due to a cooperative effect resulting from the lack of the Arg residue. This is supported by the positive-ion yields of A7, A8 and A9 as seen in Fig. 6.

It is interesting to compare the negative-ion yield of A8 (1.1%) with that of A3 (0.9%) as it demonstrates that the presence of an Asp residue at the N-terminus of A3 did not affect the ion yield. It seems that the acidic nature of the Asp residue does not contribute to an enhancement in the negative-ion yields. According to the results obtained for the corresponding free amino acids under FAB conditions using *m*NBA/DTT matrix, the acidic Asp residue should enhance the negative-ion yields. It has been reported that peptides rich in acidic residues tend to show increased signal intensity in negative-ion FAB [26]. It is important to recognize that Asp possesses both acidic and hydrophilic characteristics, because the two characteristics contribute to increase and decrease negative-ion yields, respectively. Although the acidic Asp residue probably contributes to the formation of the $[M-H]^-$ ion of A3, this effect is completely countered by their hydrophilic nature that interferes with analyte desorption from the liquid matrix. Eq. (1) is helpful to understand this complex observation. It maybe interpreted such that the acidic nature of the Asp residue enhances the ionization efficiency I, whereas the hydrophilic nature of Asp decreases the rate of desorption J_v. These two factors independently and cooperatively affect the negative-ion yields.

Among the bradykinin-related peptides, the peptides which possess an Arg residue in B4 and B5 gave higher ion yields than other peptides containing two Arg residues. In particular, the ion yield of B4 (1.2%) is significantly higher than that of B1 (0.4%). The only difference between these two peptides is the further addition of an Arg residue to the C-terminus in B4. The negative effect caused by further addition of Arg is also observed upon a comparison of B8 (0.5%) and B6 (0.1%). As described above, the negative contribution of an Arg residue on negative-ion yield is due to the preferential protonation reaction and hydrophilic nature. However, this is not the case with two Arg residues. We have reported that the presence of two Arg residues reduces the hydrophobicity of peptides, resulting in decreased ion yields in positive-ion FAB [16]. Therefore, it is likely that the negative contribution of two or more Arg residues on negative-ion yields is due to the hydrophilic nature.

The peptide ion yields in negative-ion FAB are ultimately governed by the physicochemical nature of the constituent amino acids. The presence of aliphatic/hydrophobic Leu or Ile residues seems to be advantageous for the desorption process, which may be interpreted by means of the term J_v in Eq. (1), corresponding to the rate of desorption. In contrast, aromatic/hydrophobic Phe does not play an important role in the desorption process. Although the presence of an Arg residue was effective in generation of higher ion yields in positive-ion FAB, its basic and hydrophilic nature seem to hinder the deprotonation reaction and the desorption, respectively, in negative-ion FAB.

3.5. Negative-ion yields of peptides in MALDI

Although none of the protonated angiotensin- and bradykinin-related peptides generated any fragment ions in positive-ion reflectron MALDI, some deprotonated peptides (A1, A2, A3, A4, A6, B1, B2, B3, B6, B7, B9 and B10) gave considerable abundant metastable peaks in the negative-ion reflectron MALDI mass spectra. To avoid reduction of ion yields by metastable decay, the analysis of peptides in negative-ion MALDI was performed using linear mode. The ion yields of deprotonated angiotensin- and bradykinin-related peptides in negative-ion linear MALDI are shown in Fig. 7, together with the positive-ion yields of these peptides. Among the angiotensin-related peptides, A3 (16.3%), A4 (22.1%) and A5 (22.7%) gave the highest ion yields. In contrast, A1 (7.5%), A2 (10.5%), A6 (7.3%), A7 (3.5%) and A8 (5.0%) gave relatively low ion yields. The A9 peptide did not show any molecular-related negative-ions. Among the bradykinin-related peptides, B1 (25.7%), B2 (25.5%), B3 (23.0%), B6 (21.0%), B7 (24.6%), B9 (20.6%) and B10 (22.2%) gave the highest ion yields (>20%). Other peptides gave ion yields of less than 10%.

Unlike the results obtained under FAB conditions, the positive effect of the presence of an acidic Asp residue on the yields is clearly observed under MALDI conditions. The presence of an Asp residue at the N-terminus of A3 enhanced the formation of deprotonated peptide compared to A8. Such positive influence of the Asp residue can be attributed to its acidic nature. It is likely that the presence of the Asp residue facilitates the deprotonation reaction and thus enhances the negative-ion yields. This is supported by the high negative-ion yield of acidic amino acid Asp in Fig. 5. The positive influence of Asp residues in peptides on the negative-ion yields may be interpreted *via* the term corresponding to the ionization efficiency I in Eq. (1). Comparison of the sequence of A4 and A5 indicates that conversion of Asp1 into Asn1 does not affect the ion yields (from 22.1% to 22.7%). This suggests that the role of the Asn residue on negative-ion yield of peptides is similar to the role of the Asp residue. Asn can thus also be regarded as a signal enhancing residue. It is highly unlikely that an amidic group of an Asn residue contributes to the deprotonation reaction effectively. In fact, the ion yield of Asn was lower than that of Asp (see Table 2). It is therefore likely that the amidic group of the Asn residue is advantageous for the desorption process from crystalline matrix to gas-phase.

It has been reported that Phe is advantageous in the production of gas-phase protonated peptides in positive-ion MALDI [15,16]. Here we found that Phe also enhances the negative-ion yields of peptide. Comparison of the sequences of A6 and A3 indicates that the addition of a Phe residue increased the ion yields from 7.3% to 16.3%, as shown in Fig. 7(b). Furthermore, the conversion of an aliphatic residue into an aromatic residue (Ile8 of A7 into Phe 8 of A8, Leu11 of B5 into Phe11 of B4) resulted in an enhancement of the ion yields in negative-ion MALDI. It is likely that in MALDI the yields of both protonated and deprotonated peptides are enhanced by the presence of an aromatic residue over an aliphatic residue. The trend with these results is opposite to that seen in the results obtained by

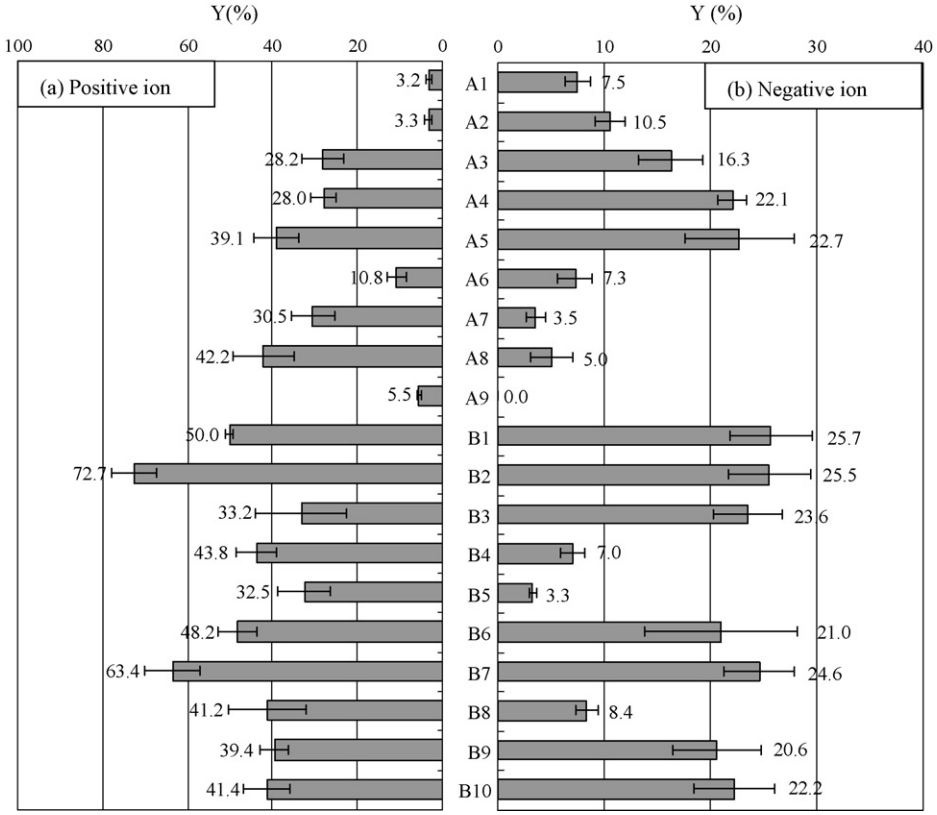

Fig. 7. Yields of molecular related ions of angiotensin-related peptides (A1–A9) and bradykinin-related peptides (B1–B10) in MALDI. (a) Yields of protonated molecules $[M+H]^+$ in positive-ion MALDI [16]. (b) Yields of deprotonated molecules $[M-H]^-$ in negative-ion MALDI.

FAB. The positive effect of aromatic residues on the yields in MALDI may be explained by the aromatic/hydrophobic residue enhancing the rate of desorption from crystalline matrix to gas-phase, and thereby increasing the ion yields in both positive- and negative-ion mode. Thus, the positive contribution of aromatic residues to the ion yields can be interpreted in terms of desorption J_v in Eq. (1).

Based on the fact that the lack of an Arg residue produced signal enhancement in negative-ion FAB, it maybe expected that the lack of an Arg residue would enhance the ion yields in negative-ion MALDI. However, the opposite results were obtained. The removal of the N-terminal Arg residue from A8 to give A9 decreased the ion yield from 5% to zero (Fig. 7(b)). The same signal decrease upon removal of the Arg residue was observed in the comparison of B1 (25.7%) and B4 (7.0%), and the comparison of B6 (21%) and B8 (8.4%). These results indicate that in negative-ion MALDI the presence of an Arg residue contributes to enhancement of the yields of deprotonated peptides. It is unlikely that the basic Arg residue is effectively deprotonated. We thus believe that the presence of an Arg residue is advantageous for desorption from crystalline matrix to gas-phase in MALDI, though a plausible mechanism is not immediately apparent. This is currently under investigation.

3.6. Molecular ion yields of peptide in ESI

Positive- and negative-ion ESI mass spectra of the peptides showed multiply protonated or deprotonated forms, $[M+nH]^{n+}$ ($n=1$–4) and $[M-nH]^{n-}$ ($n=1$–2), respectively. The ion yields in ESI were estimated as the sum of the peak areas of all charge states of the peptides. It should be noted that in LCQ ion trap instruments the detector gain is dependent on charge state and therefore the charge state distribution observed in mass spectra is not exactly the same as the charge state distribution seen with peptide ions in the ion trap [27]. The gain of the detector system increases with charge state. Since multiply protonated peptides $[M+nH]^{n+}$ have detector gains approximately n-times higher than the singly protonated peptide $[M+H]^+$, the areas of the multiply protonated peptide were divided by their charge number in order to estimate the exact charge state distribution. Likewise, this is approximately true in negative-ion ESI. Fig. 8 shows the corrected total ion yields and charge state distributions of peptides in positive- and negative-ion ESI. Although we did not use acetic acid as an additive to mobile phases in the LC system, several peptides (B2, B6, and B7) were partially detected as acetate adducts $[M+CH_3COO]^-$ in negative-ion ESI.

The charge state distributions drastically varied with sequence. Fig. 9 shows normalized charge state distributions

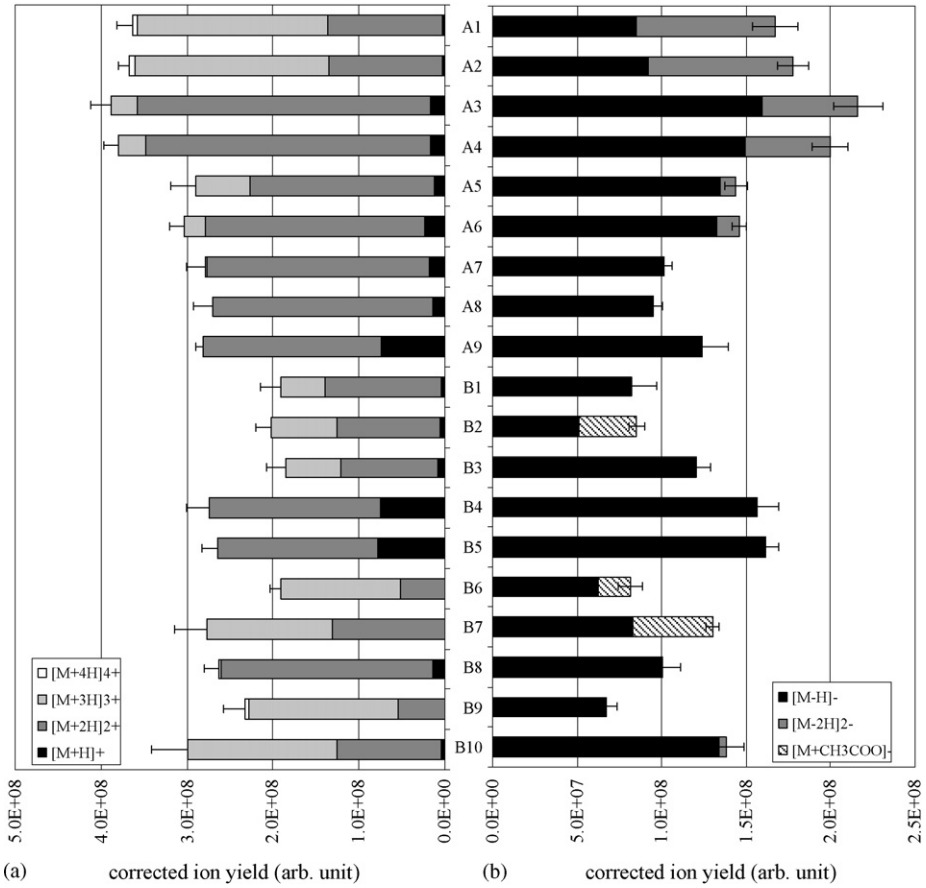

Fig. 8. Corrected total ion yields and charge state distributions of molecular related ions of angiotensin-related peptides (A1–A9) and bradykinin-related peptides (B1–B10) in ESI. (a) Yields and their charge state distributions of multiply protonated molecules $[M+nH]^{n+}$ ($n=1$–4) in positive-ion ESI. (b) Yields and charge state distributions of multiply deprotonated molecules $[M-nH]^{n-}$ ($n=1$, 2) and acetate ion adduct $[M+CH_3COO]^-$ in negative-ion ESI.

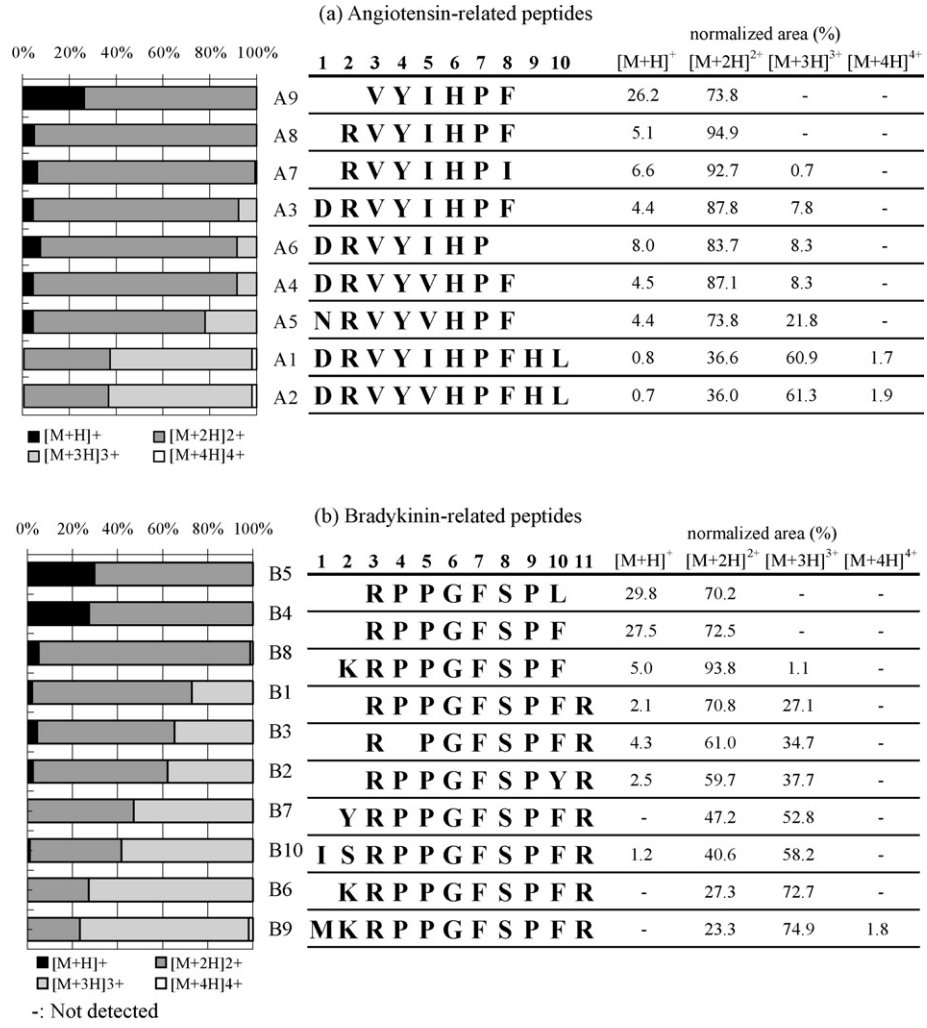

Fig. 9. Normalized charge state distributions of multiply-protonated peptides in positive-ion ESI and their amino acid sequences. (a) Angiotensin-related peptides and (b) bradykinin-related peptides.

of multiply-protonated peptides and their sequences. The peptides which contain a large number of basic sites tend to give higher charge states in positive-ion ESI. With angiotensin-related peptides, the highest charge state observed was the quadruply-protonated form $[M+4H]^{4+}$ for A1 (1.7%) and A2 (1.9%). A1 and A2 contain four basic sites at Arg2, His6, His9 and the N-terminus. The triply-protonated form $[M+3H]^{3+}$ was observed to be the dominant charge state for A1 (60.9%) and A2 (61.3%). The removal of the His-Leu portion from A1 and A2 to form A3 and A4 (Table 1) suppressed the generation of $[M+4H]^{4+}$ and $[M+3H]^{3+}$, and resulted in predominant detection of the doubly-protonated form $[M+2H]^{2+}$ (A3; 87.8% and A4; 87.1%). It is of interest to compare the charge state distribution of A8 with that of A3. Although both A8 and A3 contain three basic sites at Arg2, His6 and the N-terminus, A8 showed a lower charge state distribution than A3. The only difference between the two peptides is the removal of the Asp residue from the N-terminus of A3. The lower charge state of A8 compared to A3 can be explained by coulomb repulsion between the protonated N-terminus and the guanidinium moiety of Arg1. It is likely that it is difficult to protonate both basic sites at the same time due to coulomb repulsion. This indicates that the charge state distribution is dependent on not only the number of basic sites, but also their position within the sequence. Furthermore, A9 had a lower charge state distribution (26.2% for $[M+H]^{+}$, 73.8% for $[M+2H]^{2+}$) than A8 (5.1% for $[M+H]^{+}$, 94.9% for $[M+2H]^{2+}$). Obviously, the lack of the Arg residue from A8 is disadvantageous to multiple protonation. Similar results were obtained with bradykinin-related peptides. The highest charge state was observed as $[M+4H]^{4+}$ for B9 (1.8%). B9 contains four basic sites at Lys2, Arg3, Arg11 and the N-terminus. The $[M+4H]^{4+}$ ion disappeared after removal of Met1 from B7 to give B6. The conversion of Lys1 in B6 to Tyr1 in B7 caused increased abundance of $[M+2H]^{2+}$ (B7; 42.7%), and removal of Lys1 or Tyr1 to form B2 resulted in a lower charge state distribution of $[M+2H]^{2+}$ (59.7%) and $[M+H]^{+}$ (2.5%). From comparison of B1 and B4, it was found that removal of the C-terminal Arg9 in B1 drastically affected the charge state distribution. The formation of $[M+3H]^{3+}$ in B1 was completely suppressed by removal of Arg9 and B4 lacking Arg9 mainly gave $[M+2H]^{2+}$ (72.5%) and $[M+H]^{+}$ (27.5%). Similarly, the removal of Arg10 from B6 to form B8 altered the charge

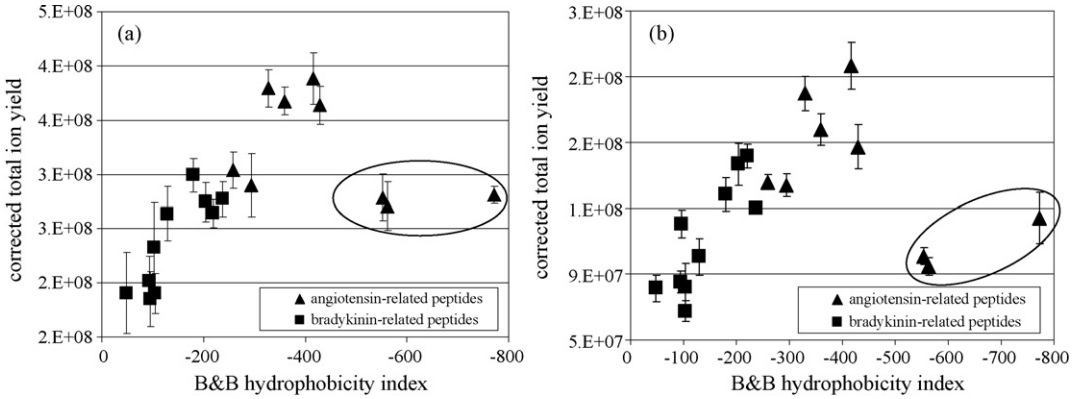

Fig. 10. Corrected total ion yields of peptides in ESI. (a) Positive-ion yields vs. hydrophobicity index and (b) negative-ion yields vs. hydrophobicity index.

state distribution. B8 gave a lower charge state distribution of $[M+3H]^{3+}$ (1.1%), $[M+2H]^{2+}$ (93.8%), and $[M+H]^{+}$ (5.0%) than B6 (72.7% for $[M+3H]^{3+}$ and 27.2% for $[M+2H]^{2+}$).

In negative-ion ESI, most peptides gave the singly-deprotonated form $[M-H]^{-}$, while some peptides (A1, A2, A3, and A4) gave abundant doubly-deprotonated form $[M-2H]^{2-}$ due to the presence of an acidic Asp residue.

The corrected total positive- and negative-ion yields of peptides were dependent on their hydrophobicity, which is directly related to surface activity, with some exceptions. The corrected total positive- and negative-ion yields of peptides as a function of their hydrophobicity indices calculated from B&B hydrophobicity [17] are shown in Fig. 10(a) and (b), respectively. Although the positive-ion yields of peptides increased with increasing hydrophobicity, the data for A7, A8, and A9 (enclosed within the ellipse in Fig. 10(a)) deviated significantly from the positive correlation. In the same way, the negative-ion yields of peptides also increased with increasing hydrophobicity, except for the data from A7, A8, and A9 (enclosed within the ellipse in Fig. 10(b)). These results can be explained as described below. It is well known that hydrophobicity, which is directly related to the surface activity, plays an important role in migration from the droplet interior to the surface and in desolvation during the electrospray process. Hydrophobic peptides therefore are advantageous for evaporation or desorption from the droplets to gas-phase, resulting in increased total positive- and negative-ion yields compared to less hydrophobic peptides. A plausible explanation for the significant deviation of the three peptides, A7, A8, and A9 from a linear correlation in Fig. 10(a) and (b) may be due to lower efficiency of the protonation or deprotonation reaction. Note that these peptides have relatively large hydrophobicities, while their charge state distributions and efficiencies of protonation or deprotonation are relatively low compared to other angiotensin-related peptides. As shown in Fig. 8, these three peptides showed lower charge state distributions than other angiotensin-related peptides in both positive- and negative-ion ESI. This indicates that the total positive- and negative-ion yields are governed not only by hydrophobicity, but also by efficiency of acquiring the charge(s). It seems that the positive contribution of hydrophobicity on the total ion yields can be interpreted in terms of desorption (J_v in Eq. (1)). In contrast, it seems reasonable to assume that the term corresponding to ionization efficiency I is related to efficiency of protonation or deprotonation, which depends upon the number of basic sites and their position in positive-ion ESI or the number of acidic sites in negative-ion ESI. As described above, the efficiency of protonation or deprotonation greatly affects the charge state distributions in ESI. The corrected total ion yields in ESI were qualitatively explicable using the concept that gas-phase ion formation requires the ionization and vaporization process just as in FAB and MALDI. In order to enhance the peptide hydrophobicity and ionization efficiency, derivatization of peptides with a reagent containing a quaternary amine with an adjacent *n*-octyl chain has been investigated [28].

4. Conclusions

In the present work, we measured the negative molecular ion yields of amino acids and peptides using FAB-MS and MALDI-MS in order to discern the factors governing the ion yields. The positive- and negative-ion yields of peptides were investigated using ESI-MS.

In FAB with *m*NBA/DTT matrix, the ion yields of amino acids were found to be dependent on gas-phase acidity and hydrophobicity. In particular, aliphatic/hydrophobicity was more efficient for producing abundant gas-phase negative-ions than aromatic/hydrophobicity. Thus, acidic amino acids (Asp and Glu) and aliphatic amino acids (Leu and Ile) gave higher negative-ion yields, while aromatic amino acids (Phe and Tyr) did not show any molecular-related negative ions. In contrast, in FAB with DEA matrix, the negative-ion yields of amino acids showed reasonable dependence on their hydrophobicity. However, aromatic amino acids gave lower ion yields than would be expected from their hydrophobicities. In MALDI, a linear correlation was observed between negative-ion yields and gas-phase acidity of amino acids. However, Arg failed to ionize despite its medium GA value, because of its outstanding basicity. This indicates that positive- and negative-ion formation occurs simultaneously and competitively. No significant correlations were observed between negative-ion yields and any other physicochemical properties including hydrophobicity.

In the analysis of peptides by both FAB and MALDI, the presence of an Asp residue contributed to enhanced negative-ion yields. In FAB, the presence of an aliphatic hydrophobic Leu or Ile residue, or alteration to Leu or Ile from other amino acid resides, tends to enhance the negative-ion yields. Similar findings have been previously reported [16], where an aliphatic/hydrophobic residue enhanced the positive-ion yields in FAB. The aliphatic/hydrophobic nature of peptides is an enhancing factor on the yields in both positive- and negative-ion FAB. In MALDI, the presence of aromatic/hydrophobic amino acid residues in peptides enhanced the negative-ion yields. It is well known that aromatic residues contribute to increases in the positive-ion yield of peptides [14–16]. Hence the aromatic/hydrophobic nature of peptides is a positive factor in production of both protonated and deprotonated peptides.

In ESI-MS, the charge state distributions of multiply-protonated peptides were dependent on the number of basic sites and their position in the sequence, while that of multiply-deprotonated peptides were also dependent on the number of acidic sites. The total ion yields of peptides were governed by hydrophobicity and efficiency of acquiring the charge(s). Ion yields of peptides under ESI conditions were also cooperatively affected by two processes, ionization and desorption, in a similar way as seen in desorption/ionization methods.

Taking these results together with those from our previous report [16], we can conclude that the ion yields of peptides are cooperatively affected by two processes, namely ionization and desorption, regardless of the ionization methods used. The ionization efficiency I in Eq. (1) can be related to thermochemical quantities such as proton affinity and gas-phase acidity, depending on the molecular-related ions such as the protonated and deprotonated form. In contrast, the rate of desorption J_v which represents the capability of analyte molecules to desorb or vaporize from condensed- to gas-phase can be related to the aliphatic/hydrophobicity in FAB, aromaticity in MALDI, and hydrophobicity in ESI, regardless of the molecular-related ions generated.

References

[1] M. Karas, D. Bachmann, U. Bahr, F. Hillenkamp, Int. J. Mass Spectrom. Ion Processes 78 (1987) 53.
[2] K. Tanaka, H. Waki, Y. Ido, S. Akita, T. Yoshida, Rapid Commun. Mass Spectrom. 2 (1988) 151.
[3] M. Karas, F. Hillenkamp, Anal. Chem. 60 (1988) 2299.
[4] C.M. Whitehouse, R.N. Dreyer, M. Yamashita, J.B. Fenn, Anal. Chem. 57 (1985) 675.
[5] J.B. Fenn, M. Mann, C.K. Meng, S.F. Wong, C.M. Whitehouse, Science 246 (1989) 60.
[6] P. Derrick, S. Patterson, Proteomics 1 (2001) 919.
[7] W.J. Henzel, T.M. Billesci, J.T. Stults, S.C. Wong, C. Grimley, C. Watanabe, Proc. Natl. Acad. Sci. U.S.A. 90 (1993) 5011.
[8] D.J.C. Pappin, P. Hojrup, A.J. Bleasby, Curr. Biol. 3 (1993) 327.
[9] M. Mann, M. Wilm, Anal. Chem. 66 (1994) 4390.
[10] J.K. Eng, A.L. McCormack, J.R. Yates, J. Am. Soc. Mass Spectrom. 5 (1994) 976.
[11] P.M. Bigwarfe Jr., T.D. Wood, Int. J. Mass Spectrom. 234 (2004) 185.
[12] K. Janek, H. Wenschuh, M. Bienert, E. Krause, Rapid Commun. Mass Spectrom. 15 (2001) 1593.
[13] E. Krause, H. Wenschuh, P.R. Jungblut, Anal. Chem. 71 (1999) 4160.
[14] M.L. Valero, E. Giralt, D. Andreu, Lett. Peptide Sci. 6 (1999) 109.
[15] S. Baumgart, Y. Lindner, R. Kühne, A. Oberemm, H. Wenschuh, E. Krause, Rapid Commun. Mass Spectrom. 18 (2004) 863.
[16] T. Nishikaze, M. Takayama, Rapid Commun. Mass Spectrom. 20 (2006) 376.
[17] H.B. Bull, K. Breeze, Arch. Biochem. Biophys. 1621 (1974) 665.
[18] K.E. Colyer, C.M. Jones, R.A. Metz, A.K. Pawlow, E.D. Wischow, J.C. Poutsma, Proceedings of the 54th ASMS Conference on Mass Spectrometry and Allied Topics, Seattle, 2006, TP 145.
[19] R.A.J. O'Hair, J.H. Bowie, S. Gronert, Int. J. Mass Spectrom. 117 (1992) 23.
[20] S. Naylor, A.F. Findeis, B.W. Gibson, D.H. Williams, J. Am. Chem. Soc. 108 (1986) 6359.
[21] R.M. Caprioli, W.T. Moore, G. Petrie, K. Wilson, Int. J. Mass Spectrom. Ion Processes 86 (1988) 187.
[22] G.M. Allmaier, C.E. Costello, Rapid Commun. Mass Spectrom. 2 (1988) 74.
[23] R. Wang, L. Chen, R.J. Cotter, Anal. Chem. 62 (1990) 1700.
[24] P. Pucci, C. Sepe, G. Marino, Biol. Mass Spectrom. 21 (1992) 22.
[25] M.V. Kosevich, V.S. Shelkovsky, O.A. Boryak, V.V. Orlov, Rapid Commun. Mass Spectrom. 17 (2003) 1781.
[26] A.M. Buko, L.R. Phillips, B.A. Fraser, Biomed. Mass Spectrom. 10 (1983) 387.
[27] J.C. Schwartz, S.T. Quarmby, A.E. Schoen, Proceedings of the 46th ASMS Conference on Mass Spectrometry and Allied Topics, Orlando, 1998, p. 484.
[28] H. Mirzaei, F. Regnier, Anal. Chem. 78 (2006) 4175.